Temperature and Angular Dependence of the Magnetoresistance in Low Dimensional Organic Metals

J. S. Qualls[1], J. S. Brooks[2], S. Uji [3], T. Terashima[3], C. Terakura[3], H. Aoki[3], L. K. Montgomery [4]

[1] *Wake Forest University, Winston-Salem, NC 27109, USA*

[2] *National High Magnetic Field Laboratory, Florida State University, Tallahassee, FL 32306, USA*

[3] *National Research Institute for Metals, Tsukuba, Ibaraki 305, Japan*

[4] *Department of Chemistry, Indiana University, Bloomington, IN 47405, USA*

Abstract

Detailed studies of the magnetoresistance of α-$(ET)_2KHg(SCN)_4$ and α-$(ET)_2TlHg(SCN)_4$ as a function of temperature, magnetic field strength, and field orientation are reported. Below 15 K, the temperature dependence of the magnetoresistance is metallic ($dR/dT > 0$) for magnetic field orientation corresponding to an angular dependent magnetoresistance oscillation (AMRO) minimum and nonmetallic ($dR/dT < 0$) at all other field orientations. We find that this behavior can be explained in terms of semiclassical models without the use of a non-Fermi liquid description. The alternating temperature dependence (metallic/nonmetallic) with respect to field orientation is common to any system with either quasi-one or two-dimensional AMRO. Furthermore, we report a new metallic property of the high field and low temperature regime of α-$(ET)_2MHg(SCN)_4$ (where M = K, Rb, or Tl) compounds.

I. INTRODUCTION

Recently, non-Fermi liquid behavior has been proposed to describe transport properties of the quasi-one-dimensional organic conductor $(TMTSF)_2PF_6$. [1–5] This assignment is based on the temperature and angular dependence of the magnetoresistance in tilted magnetic fields. A characteristic signature of the angular dependent magnetoresistance of $(TMTSF)_2PF_6$ is its oscillatory nature, where at "magic angles" the resistance exhibits sharp dips against a broad $cos(\theta)^\gamma$ background. [6,7] This feature is thought to arise from the warped open orbit Fermi surface sheets. As the field strength is increased along the second most conducting **b** axis, the effective electronic dimensionality is decreased. For temperatures below $\approx$ 20 K this reduction in dimensionality leads to a decoupling of the layers (or a loss of phase coherence for electronic states between planes), i.e. non-Fermi liquid behavior and a nonmetallic ($dR/dT < 0$) temperature dependence. [3,5] Below 8 K, for fields orientations generating dips in the magnetoresistance, a metallic ($dR/dT > 0$) temperature dependence is recovered. Away from the magic angles the temperature dependence changes slightly, however it remains non-metallic ($dR/dT < 0$). This metallic/nonmetallic behavior is explained in terms of a restoration of the interplane coupling at the magic angles and a second decoupling at all other orientations due to fields along the **c** axis. [3,5]

Similar to $(TMTSF)_2PF_6$, the material α-$(ET)_2KHg(SCN)_4$ displays angular dependent magnetoresistance oscillations (AMRO) and metallic/non-metallic temperature dependence of the magnetoresistance. Does this indicate that α-$(ET)_2KHg(SCN)_4$ experiences non-Fermi liquid transport? If not, what is the relationship between the temperature dependence and AMRO?

At room temperature, α-$(ET)_2MHg(SCN)_4$, where M = K, Tl, or Rb has a Fermi surface defined by the coexistence of a quasi-two-dimensional cylinder and quasi-one-dimensional sheets. [8,9] By decreasing the temperature, a Fermi surface reconstruction occurs at T_{DW} (where T_{DW} = 8 K, 10 K, or 12 K, for M = K, Tl, or Rb respectively) and a new electronic ground state develops. [10] The true nature of the low temperature ground state is a subject of contemporary debate, however approaches assuming a charge density wave framework

appear very promising. [11–14] Figure 1 is a schematic $B-T$ phase diagram for the α-$(ET)_2KHg(SCN)_4$ compound. [11,15] For the field perpendicular to the most conducting plane, the electronic structure can be separated into three regimes; the normal state, density wave one (DWI), and density wave two (DWII). Evidence of a third phase has been observed for field orientations near the most conducting plane. [14] The electronic structure of this new phase appears to be very similar to that of DWI. To simplify the following arguments it will not be examined in this work. Each electronic regime of α-$(ET)_2KHg(SCN)_4$ has its own characteristic dependence of the magnetoresistance with respect to field orientation, which is indicated in Fig. 1 as either quasi-one or quasi-two-dimensional. At low temperatures, a characteristic "one-dimensional" angular dependent magnetoresistance is observed, with dips against a broad $cos(\theta)^\gamma$ background similar to $(TMTSF)_2PF_6$. [16–20] On the other hand, at high temperature and fields a characteristic "two-dimensional" angular dependent magnetoresistance, with peaks periodic in $\tan(\theta)$is observed. [10,21] A similar $B-T$ phase diagram is found in the M = Tl and Rb compounds as well.

In this work, we examine the temperature dependence of the magnetoresistance of α-$(ET)_2KHg(SCN)_4$ and α-$(ET)_2TlHg(SCN)_4$ as a function of field orientation. Although the compounds are characterized by a complex ground state which is field and temperature dependent, we find that many aspects of a standard, semi-classical Boltzmann treatment provide a good account of the data without invoking unconventional transport mechanism. From the temperature dependence of the magnetoresistance, two features are evident. The first feature is common to these materials and to any system exhibiting angular dependent magnetoresistance oscillations (AMRO). By applying a magnetic field, a nonmetallic behavior results in the temperature dependence of the magnetoresistance at low temperatures (this behavior is not indicative of a phase transition or non-Fermi liquid behavior). Based on the specific electron trajectories along the warped Fermi surface, there is an effective reduction of the electronic dimensionality. The angular dependence of the electronic dimensionality is reflected in the field and temperature dependence of the magnetoresistance. By changing the field orientation, the temperature dependence of the magnetoresistance oscillates between

that of metallic ($dR/dT > 0$) at AMRO minima and nonmetallic ($dR/dT < 0$) at AMRO maxima. Because AMRO effects only appear at temperatures below $\approx$ 15 K, we will restrict the temperature range to 25 K and below. The second feature is an angular dependent metallic behavior observed in α-$(ET)_2KHg(SCN)_4$ and α-$(ET)_2TlHg(SCN)_4$ inside of DWII.

II. REVIEW OF SEMICLASSICAL FORMALISM

For a general anisotropic metal, Fermi liquid theory predicts the phonon scattering rate, $1/\tau_p$, to be proportional to $T^2/t_\perp$, where $t_\perp$ is the transfer integral in transverse direction. The electron-electron scattering rates change with dimensionality. For three dimensions $1/\tau_u$ is expected to be proportional T^2/E_F, for two dimensions proportional to $(T^2/E_F)ln(E_F/T)$ and for one dimension proportional to T^2/t_b, with E_F being the Fermi energy. [23] Although exact details of the Fermi surface and scattering mechanism (Umklapp, phonon, or defect)in α-$(ET)_2KHg(SCN)_4$ is debatable, we can approximate τ based on the temperature dependence of the resistance, where $\sigma_{ZZ} \propto constant \times \tau$. At zero fields, the resistance of α-$(ET)_2MHg(SCN)_4$ exhibits a metallic behavior at low temperatures (see Fig. 2). Inside the normal metallic state, the resistance is proportional to the temperature, $R(T) = A_1 + A_2T$, where A_i are constants. Inside of DWI,$R(T) = A_3+A_4T+A_5T^2$. Note the similarity between R(T) in DWI and in $(TMTSF)_2PF_6$ ($R(T) \propto T^2$). [23] By solving the semiclassical Boltzmann transport equation [24], for the specific energy dispersion relation, the observed AMRO features are reproduced for both quasi-one and two-dimensional systems. [16,17,25–31] From the calculated conductivity, the temperature dependence can be predicted at specific field orientations and can be summarized as following.

Quasi-one-dimensional The assumed quasi-one-dimensional energy band dispersion for a pair of warped Fermi sheets is $\varepsilon_k = \hbar v_F(|k_x| - k_F) - (\sum_{m,n}[t_{mn}^{even} cos(\mathbf{R}_{mn} \cdot \mathbf{k}_\parallel) + t_{mn}^{odd} sin(\mathbf{R}_{mn} \cdot \mathbf{k}_\parallel)]$, where $t_{m,n}$ is the transfer integral associated with the oblique lattice vector $\mathbf{R}_{mn} = (0, mb+nd, nc)$ and describes the warping topology. [25] The conductivity for field rotations in the plane of the Fermi sheets as generated by the semiclassical Boltzmann equation can be written as [25]:

$$\sigma_{ZZ} = N(\varepsilon_F) \sum_{m,n}^{\infty} \left(\frac{et_{m,n}}{\hbar}\right)^2 n^2 c^2 \frac{\tau}{1 + (G_{m,n}\nu_F\tau)^2}, \quad (1)$$

where $N(\varepsilon_F)$ is the density of states at the Fermi level per unit volume, τ is the scattering time, $G_{m,n} = eB((mb+nd)cos\theta - ncsin\theta)/\hbar$, B is the magnetic field, e is the electron charge, and ν_F is the Fermi velocity. The $G_{m,n}$ term contains the field dependence of σ_{ZZ}.

Although no semiclassical prediction for the temperature dependence of the magnetoresistance in a quasi-one-dimensional case has been made, it is easily derived. When the field orientation is aligned at AMRO minima, $G_{m,n}$, vanishes and the conductivity is simply $\sigma_{ZZ} = constant \times \tau = constant' \times \sigma_{ZZ}(B = 0)$, resulting in a temperature dependence of the resistivity being metallic(dR/dT > 0). On the other hand, at AMRO maxima, $G_{m,n}$ dominates and the conductivity can be written as $\sigma_{ZZ} = 1/(G_{m,n}\nu_F)^2\tau$. The resulting temperature dependence of the resistivity at AMRO maximum is proportional to τ and is nonmetallic(dR/dT < 0). From the zero field data we know that in the DWI state that $1/\tau$ is proportional to R(T), we can easily predict the temperature dependence of the resistivity; at AMRO maxima $R(T) \propto 1/(a_1T + a_2T^2)$, and at AMRO minima $R(T) \propto a_3T + a_4T^2$, where a_i are constants. Furthermore, $G_{m,n}$ has a linear field dependence. As the magnetic field strength increases, the resistance at AMRO maxima will increase, whereas the magnetoresistance at the AMRO minima will be almost field independent. Thus by increasing the field strength the metallic/non-metallic behavior becomes more pronounced.

Quasi-two-dimensional The assumed quasi-two-dimensional energy band dispersion for a corrugated Fermi cylinder is $\varepsilon_k = \hbar^2(k_x^2 + k_y^2)/2m^* - 2t_z cos(ck_z)$. Here k_x and k_y are the components of the wave vector **k** in the conducting-plane, c is the inter-plane distance, k_z is the wave vector component normal to the planes, and m* is the effective cyclotron mass in the conducting plane. The interlayer transfer integral t_z is small compared to the Fermi energy such that $\varepsilon_F/t_z \gg 1$, generating a slightly warped cylindrical Fermi surface. By solving the Boltzmann equation, the conductivity (or resistivity) along the least conductive axis can now be calculated. When the field is sufficiently high or the temperature is sufficiently low, $\omega_o\tau cos(\theta_{max}) >> 1$, where ω_o is the cyclotron frequency, eB/m^*, then at AMRO maximum

the normalized resistivity can be written as [29]:

$$\frac{\rho_{zz}(\theta_{AMROmax})}{\rho_{zz}(B=0)} = \frac{\gamma(\omega\tau)^2 sin(2\theta_{AMROmax})}{\pi}. \tag{2}$$

The resulting temperature dependence of the resistivity at AMRO maximum is proportional to τ and is nonmetallic (dR/dT < 0).

At the AMRO minimum, the normalized resistivity can be written as [29]:

$$\frac{\rho_{zz}(\theta_{AMROmin})}{\rho_{zz}(B=0)} = \frac{\pi^2}{2}\left(n+\frac{1}{4}\right), \tag{3}$$

where n is an integer. The temperature dependence of the resistivity at AMRO minima is proportional to $1/\tau$ and metallic(dR/dT > 0). The temperature dependence has approximately the same behavior as in the quasi-one-dimensional case, however in this case $1/\tau$ is proportional to T instead of $T + T^2$.

The above discussion is also understandable in a rather intuitive way. By changing the field orientation, the electron trajectories along the warped Fermi surface also change. For specific field orientations the velocity is more effectively averaged to zero and transport is reduced. For the Fermi cylinder, the velocity vector along the cylinder axis goes to zero when all closed orbits share the same area. For the Fermi sheets, the velocity vector is reduced when the electrons are not traveling along the axis of corrugation. Thus, the effective dimensionality oscillates with field orientation. At AMRO maximum the system has reduced dimensionality and at AMRO minimum the dimensionality is restored.

III. EXPERIMENT

Single crystals of α-(ET)$_2$MHg(SCN)$_4$, where M = K or Tl, were grown using conventional electrocrystallization techniques. [10] Systematic measurements of the temperature dependence of the magnetoresistance from 30 K to 1.5 K at various field orientations and strengths were performed in the 33 tesla resistive magnet at NHMFL, Tallahassee. The magnetoresistance was measured using standard four terminal AC techniques with 12 μm gold wires attached via graphite paste. The current was applied along the least conducting $\mathbf{b}^\star$ axis. Typical contact resistance was below 10 Ω. Samples were rotated in magnetic

field with θ being defined as the angle between the $\mathbf{b}^\star$ axis and field. The field projection angle(ϕ) with respect to the $\mathbf{a}-\mathbf{c}$ plane was determined via polarized infrared reflectance. The magnetic field was oriented $\approx 8^\circ$ from the $\mathbf{c}$ axis in the M = K sample and $\approx 30^\circ$ from $\mathbf{c}$ axis in the M = Tl sample.

IV. RESULTS

A. Temperature dependence in DWI

AT 14 T the electronic state is well inside DWI. Typical AMRO for this regime is shown in Fig. 3(a). The oscillations are characterized by minimum periodic in $\tan(\theta)$ and a maximum when the field is near the $\mathbf{b}^\star$ axis. [16–20] The background magnetoresistance can be fit to $cos(\theta)^\gamma$, where γ varies from 0.6 to 1.6 based on sample quality and field strength. The AMRO is very similar to that observed in $(TMTSF)_2PF_6$ where the background magnetoresistance can be fit to $cos(\theta)^\gamma$, where $\gamma\approx 0.5$, [7] however the dips in $(TMTSF)_2PF_6$ are not as deep as in α-$(ET)_2MHg(SCN)_4$. The temperature dependence of the magnetoresistance for different field orientations for α-$(ET)_2KHg(SCN)_4$ are shown in Fig. 3(b). When the field direction corresponds to an AMRO minimum, the sample resistance is metallic ($dR/dT > 0$) (see Fig. 3(b) curve D). Deviations from this orientation results in nonmetallic ($dR/dT < 0$) behavior in the temperature dependence. This nonmetallic behavior becomes more pronounced as the field orientation approaches AMRO maxima (curves C, B, and then A). In some samples the nonmetallic behavior, occurring at AMRO maxima saturates at very low temperatures. This saturation of the magnetoresistance arises due to impurities or lattice defect scattering and indicates the limit at which the dimensionality can be reduced.

Figure 4 is a plot of the temperature dependence of the magnetoresistance in α-$(ET)_2KHg(SCN)_4$ at AMRO maximum and minimum (as indicated in Fig. 3) in a wide temperature range. The onset of DWI is very clear. The data is represented by open circles and the fits by solid lines. The fits are obtained from the semiclassical Boltzmann treatment described in the previous section and using the zero field temperature dependence to determine $1/\tau$ (AMRO minimum fit to $A_1 + A_2T + A_3T^2$ and AMRO maximum fit to

$A_4/(A_5 + A_6T + A_7T^2)$, where A_i are constants). At field orientations corresponding to AMRO maximum, the sample resistance is proportional to a $1/(a_1T + a_2T^2)$ dependence. At field orientations corresponding to AMRO minimum, the temperature dependence of the resistance is the same as that realized at zero fields and is proportional to the temperature, $a_3T + a_2T^4$, where a_i are constants.

Although the angular dependent magnetoresistance oscillations can be reproduced via semiclassical descriptions, there are still some complications to be addressed. It has been shown that the magnetoresistance violates Kohler's rule in DWI, thus indicating that semiclassical methods may not be valid. [32] It is likely that there are additional complications such as magnetic breakdown, electronic subphases, or mixed states inside of DWI.

Another approach to explain AMRO in the DWI of α-$(ET)_2KHg(SCN)_4$ considers incoherent transport. [33] Albeit this approach is not strictly semiclassical, it is included for completeness. In this model the reconstructed Fermi surface of DWI is not characterized by a quasi-one-dimensional but a quasi-two-dimensional topology. In fact, one of the proposed models for the reconstructed Fermi surface inside of DWI has the Fermi surface characterized by cylinders instead of sheets. The alternative model for the angular dependent magnetoresistance can be summarized in the following way. When a magnetic field is applied to a density wave structure, a resulting periodic potential is created in the inter-plane direction. As the field direction is rotated, this periodicity changes. If the periodicity becomes commensurate with the interlayer spacing, the electron states are extended. This corresponds to AMRO minima. At the minima, the electronic system is metallic and the sample resistance should decrease with decreasing temperatures. When the inter-plane potential is not commensurate to the interlayer spacing the magnetoresistance increases. When the potential is exactly out of phase with the interlayer spacing the system now corresponds to AMRO maxima. In this orientation, the electron wave function begins to shrink and localize with increasing field or decreasing temperature, resulting in incoherent electron motion. In this field orientation, the sample resistance should increase with decreasing temperature. Unfortunately, no specific predictions for the functional form of the temperature dependence have

been made yet for this model.

B. Temperature dependence in the normal metal state

At 30 and 33 tesla, α-$(ET)_2MHg(SCN)_4$ is in the normal state except for angles $\theta \geq 80°$ and for temperatures below ≈ 3 K (inside DWII). Figure 5 (left side) displays typical quasi-two-dimensional AMRO as observed in the normal metal state and DWII. The oscillations are characterized by maxima periodic in $\tan(\theta)$ with the first minimum occurring near $\theta = 0 \pm 6°$. [34] We have measured the temperature dependence of R(T) at many field orientations. The solid arrows indicate field orientations (E, F, G, and H as shown in Fig. 5 right side) where the temperature dependence of the magnetoresistance was measured. Unfortunately, Shubnikov-de Haas (SdH) oscillations dominate as the sample is rotated in high magnetic fields. [35] The SdH oscillations are superimposed on top of the angular dependent magnetoresistance oscillations. If the field orientation corresponds to either SdH maximum or minimum, an additional term will appear in the temperature dependence of the magnetoresistance. Therefore field orientations corresponding to SdH minimum or maximum will be omitted in the following discussion by avoided angles near θ=0°.

Inside the normal state we find that when the field is aligned along AMRO minimum, the temperature dependence of the magnetoresistance is metallic($dR/dT > 0$) (see right side Fig. 5 curve H). Deviations from field directions corresponding to precise minimum position results in a change of the temperature dependence ($dR/dT < 0$). This nonmetallic behavior is more pronounced near AMRO maximum (see right side Fig. 5 curves G, F, and then E). Although the AMRO has changed its form, the temperature dependence is very similar to Fig. 3 and 4.

The temperature dependence of the magnetoresistance at the AMRO maximum and AMRO minimum is displayed in Fig. 6 (the field orientations are indicated in Fig. 5). The solid lines are fits (AMRO minimum fit to $A_1T + A_2$ and AMRO maximum fit to $A_3/(A_4T+A_5T^2)$, where A_i are constants). Like inside DWI the temperature dependence is described by semiclassical Boltzmann treatment. Deviations to the fit begin to occur at lowest temperatures as DWII and a new metallic behavior sets in (see Fig. 5 curve E).

At first glance one might believe that the nonmetallic like behavior is resulting from a gap opening. Yet, the behavior of the temperature dependence can be explained in terms of semiclassical transport. At AMRO maximum, the system is more effectively two dimensional with increasing field strength or decreasing temperature. All quasi-two-dimensional systems exhibiting AMRO will experience nontrivial temperature dependence.

C. Temperature dependence in DWII

When the magnetic field orientation is close to AMRO maxima a new behavior is observed at high fields and low temperatures in the temperature dependence of the magnetoresistance. There is a transition from a non-metallic to a metallic behavior at a transition temperature T_M (see right side Fig. 5 curve E). This reentrant metallic behavior is a signature of the DWII regime. In one sample of α-$(ET)_2TlHg(SCN)_4$, T_M was ≈ 4 K and could be observed at many angles, especially near AMRO maxima. Figure 6 shows the evolution of the slope and T_M with respect to θ at 30 and 33 T. Once inside DWII, both the magnetoresistance and the magnetization drop abruptly, however, the mechanism responsible for the behavior is questionable. [15,36] From AMRO and Shubnikov-de Haas measurements, the Fermi cylinders of the normal state are clearly observed within DWII, [21] suggesting that the Fermi surface is very similar to that of the normal state. The replacement of the nonmetallic behavior by the metallic one indicates the existence of a new unidentified property of DWII, and may be related to the appearance of large eddy currents observed in previous experiments within the DWII regime. [37–39]

If we assume the electronic conduction in DWII is due to the normal state plus that of another highly conductive transport channel, we are able to fit the measured data. Two contributions, one due to the original Fermi surface (an angular dependent term $\propto 1/T$) and the other due to the new metallic term (an angular independent term $\propto T$), are added in parallel. The fits are shown in Fig 6(b). This reproduces the observed behavior and describes the dependence of T_M on field orientation and strength. The slope of the temperature dependence of the magnetoresistance will also be greater at AMRO maximum. This is because there is a significant difference in the magnetoresistance between the AMRO maximum and

minimum (see left side Fig. 5). The origin of this new metallic term is not clear. A possible explanation is a transfer of carriers from the original quasi-two dimensional Fermi surfaces to another conduction channel. By removing carriers from the cylinders, yet retaining them on some other Fermi surface, there is an increase of dimensionality and conductivity. Could it indicate the existence of highly conductive edge states or the emergence of a new Fermi surface? With the onset of DWII, the Fermi surface reconstructs and the effects of the original Fermi surface are being suppressed (including the nonmetallic behavior). At high fields or specific field orientations, the nesting condition may improve such that more carriers are transferred from the original Fermi surface. Further investigations of this unusual phase are required.

V. SUMMARY

We have investigated the effects of field strength and orientation on the temperature dependence of the magnetoresistance in samples of α-$(ET)_2MHg(SCN)_4$ (M = K or Tl). At angular dependent magnetoresistance oscillation (AMRO) minima the temperature dependence is metallic and at AMRO maxima the magnetoresistance shows nonmetallic temperature dependence. When the magnetic field is oriented along AMRO maxima, the effective electronic dimensionality decreases with decreasing temperature and increasing field. We show that non-Fermi liquid transport is not necessary to generate an angular dependent temperature dependence. This behavior can be explained in terms of semiclassical electron transport and the Boltzmann equation. Although the scattering rates for every system will be different based on details of the Fermi surface and what not, the metallic/nonmetallic temperature dependence of the magnetoresistance should be common to any low dimensional system with AMRO.

The temperature dependence of the magnetoresistance at different fields (for fixed angle) reported by Ref. [15] and Ref. [12] on α-$(ET)_2KHg(SCN)_4$ can also be explained in terms of semiclassical theory. In the first reference the field is oriented at an AMRO minimum in DWI and an AMRO maximum in the normal state (see Fig. 1 Ref. [15]). The temperature dependence of the magnetoresistance is non-metallic in the normal state, and metallic in

DWI and DWII. In the second reference, Ref. [12] the field is oriented near θ=0° or at an AMRO maximum in DWI and at an AMRO minimum in the normal state. The temperature dependence of the magnetoresistance is metallic in DWII, however there is a nonmetallic behavior in DWI *and* the normal state. Albeit the effect is less pronounced in later measurements by the same author, the nonmetallic behavior in the normal state is reproduced(at the same field orientation). It is not known if this is an effect particular to $\theta \approx 0°$ or not. The field orientation may not have been along the precise AMRO minimum. If the sample is slightly misalign or the first AMRO minimum is not at θ= 0° (there is a range of ± 6° based on the ϕ field orientation in the conducting plane), the sudden rise before DWII state would correspond to the non-metallic behavior observed when away from precise AMRO minima.

A quasi-one-dimensional organic charge transfer salt $(TMTSF)_2PF_6$ exhibits a very similar temperature dependent magnetoresistance as that in the low temperature regime of α-$(ET)_2MHg(SCN)_4$. [5] The temperature dependence of $(TMTSF)_2PF_6$ has been modeled extensively in terms of non-Fermi liquid transport. It would be interesting to test semiclassical models on this temperature dependence to see if non-Fermi liquid behavior is required.

To first order, the transport in all regimes of α-$(ET)_2MHg(SCN)_4$ can be understood in terms of semiclassical orbits(using both quasi-one and quasi-two-dimensional models). This semiclassical approach leads, naturally, to a nonmetallic behavior at all maxima in angular dependent magnetoresistance oscillations due to a reduction of the effective electronic dimensionality with increasing magnetic field or decreasing temperature. Furthermore, a new metallic property of DWII is reported. The mechanism responsible for this metallic behavior is unknown and the nature of the DWII phase will be the subject of future investigations.

ACKNOWLEDGMENTS We would like to thank L. Balicas, S. Y. Han, and B. H. Ward for useful discussions. This work was supported by the National Science Foundation under Grant No. NSF-DMR-99-71474.

REFERENCES

[1] G. Kriza, G. Szeghy, I. Kézsmárki, and G. Mihály, Phys. Rev. B **60**, 8434 (1999).

[2] S.P. Strong, D. G. Clark, and P. W. Anderson, Phys. Rev. Lett. **73**, 3714 (1994) ;D. G. Clarke and S. P. Strong, Adv. Phys. **46**, 545 (1997).

[3] A. T Zhelezynyak and V. M. Yakovenko, cond-mat/9802172v2(unpublished).

[4] A. G. Lebed, J. Phys. I France **6**, 1819 (1996).

[5] E.I. Chashechkina and P. M. Chaikin, Phys. Rev. Lett. **80**, 2181 (1998).

[6] T. Osada, A. Kawasumi, S. Kagoshima, N. Miura, and G. Saito, Phys. Rev. Lett. **66**, 1525 (1991).

[7] W. Kang, S. T. Hannahs, and P. M. Chaikin, Phys. Rev. Lett. **69**, 2827 (1992).

[8] H. Mori, S. Tanaka, M. Oshima, G. Saito, T. Mori, Y. Murayama, and H. Inokuchi, Bull. Chem. Soc. Jpn. **63**, 2183 (1990).

[9] L. Ducasse and A. Fritsch, Solid State Comm. **91**, 201 (1994).

[10] T. Ishiguro, J. Yamaji, and G. Saito, in *Organic Superconductors*, (Springer-Verlag, Berlin, Heildeberg, New York,1998); J. Wosnitza, *Fermi Surfaces of Low-Dimensional Organic Metals and Superconductors*, (Springer-Verlag, Berlin, Heildeberg, New York,1996).

[11] N. Biškup, J. A. A. J. Perenboom, J. S. Brooks and J. S. Qualls, Solid State Comm. **107**, 503 (1998); M. V. Kartsovnik *et al.*, Synth Met. **86**, 1933 (1997).

[12] T. Sasaki, A. G. Lebed, T. Fukase, and N. Toyota, Phys. Rev. B. **54**, 12969 (1996); T. Sasaki, T. Fukase, N. Toyota, Physica B **216**, 366 (1996).

[13] R. H. McKenzie, cond-mat/9706235 (1997).

[14] J. S. Qualls, L. Balicas, J. S. Brooks, N. Harrison, L. K. Montgomery, and M. Tokumoto,

submitted to Phys. Rev. Lett. (unpublished).

[15] M. V. Kartsovnik, W. Biberacher, E. Steep, P. Christ, K. Andres, A. G. M. Jansen, and H. Muller, Synth. Metals **86**, 1933 (1997).

[16] T. Osada, R. Yagi, A. Kawasumi, S. Kagoshima, N. Miura, M. Oshima, and G. Saito, Phys. Rev. B **41**, 5428 (1990); T. Osada, R. Yagi, A. Kawasumi, S. Kagoshima, N. Miura, M. Oshima, H. Mori, T. Nakamura, and G. Saito, Synth. Metals **41-43**, 2171 (1991).

[17] Y. Iye, R. Yagi, N. Hanasaki, S. Kagoshima, H. Mori, H. Fujimoto, and G. Saito, J. Phys. Soc. Jpn. **63**, 674 (1994);Physica B **201**, 474 (1994); T. Sasaki and N. Toyota, Phys. Rev. B **49**, 10120 (1994); Physica B **201**, 466 (1994); Synth. Metals **70**, 849 (1995).

[18] J. Caulfield, J. Singleton, P. T. J. Hendriks, J. A. A. J. Perenboom, F. L. Pratt, M. Doporto, W. Hayes, M. Kurmoo, and P. Day, J. Phys. Condens. Matter **6**, L155 (1994).

[19] A. E. Kovalev, M. V. Kartsovnik, R. P. Shibaeva, L. P. Rozenberg, I. F. Schegolev, and N. D. Kushch, Solid State Commun. **89**, 575 (1994); V. Kartsovnik, A. E. Kovalev, R. P. Shibaeva, L. P. Rozenberg, and N. D. Kushch, Physica B **201**, 459 (1994).

[20] V. Kartsovnik, A. E. Kovalev, and N. D. Kushch, J. Phys. I France bf 3, 1187 (1993).

[21] for a review see A. A. House, S. J. Blundell, M. M. Honold, J. Singleton, J. A. A. J. Perenboom, W. Hayes, M. Kurmoo, and P. Day, J. Phys. Condens. Matter **8**, 8829 (1996).

[22] J. S. Brooks, G. J. Athas, S. J. Klepper, X. Chen, C. E. Campos, S. Valfells, Y. Tanaka, T. Kinoshita, N. Kinoshita, M. Tokumoto, and H. Anzai, Physica B **201**, 449 (1994).

[23] L. P. Gor'kov, M. Mochena, Phys. Rev. B **57**, 6204 (1998).

[24] J. M. Ziman, *Principles of the Theory of Solids* (Cambridge University Press, Cambridge

1972).

[25] S. J. Blundell and J. Singleton, J. Phys. I France **6**, 1837 (1996); Phys. Rev. B **53**, 5609 (1996).

[26] T. S. Osada, S. Kagoshima, and N. Miura, Phys. Rev. B **46**, 1812 (1992).

[27] R. Yagi and Y. Iye, Solid State Commun. **89**, 275 (1994); J. Phys. Soc. Jpn. **59**, 3069 (1990).

[28] G. M. Danner, W. Kang, and P. M. Chaikin, Phys. Rev. Lett. **72**, 3714 (1994).

[29] P. Moses and R. H. McKenzie, Phys. Rev. B **60**, 7998 (1999).

[30] A. J. Shofield, J. R. Cooper, and J. M. Wheatley, cond-mat/9709167.

[31] V. G. Peschansky, J. A. R. Lopez, and T. G. Yao, J. Phys. I France **1**, 1469 (1991).

[32] R. H. McKenzie, J. S. Qualls, S. Y. Han, and J. S. Brooks, Phys. Rev. B **57**, 11854 (1998).

[33] D. Yoshioka, J. Phys. Soc. Jpn. **64**, 3168 (1995).

[34] K. Yamaji, J. Phys. Soc. Jpn. **58**, 1520 (1989).

[35] D. Shoenberg, *Magnetic Oscillations in Metals*, (Cambridge University Press, Cambridge 1984).

[36] P. Christ, W. Biberacher, H. Muller, K. Andres, E. Steep, and A. G. M. Jansen, Physica B **204**, 153 (1995).

[37] M. M. Honold, N. Harrison, P. Day, J. Phys. Condens. Matter **9**, 533 (1997).

[38] N. Harrison , A. House, M. V. Kartsovnik, A. V. Polisski, J. Singleton, F. Herlach, W. Hayes, and N. D. Kushch, Phys. Rev. Lett., **77**, 1576 (1996).

[39] H. Yaguchi, N. Harrison, P. Day, Physica B **249-251**, 75 (1998).

FIGURES

FIG. 1. Schematic phase diagram and AMRO behavior in the M = K salt. The diamonds [12] and circles [11] indicate the transition into the low temperature ground state from transport measurements. The triangles signify the kink field, B_K and separate DWI from DWII. The light gray, and dark gray color corresponds respectively to regions of quasi-two-dimensional or quasi-one-dimensional. For the hysteretic regions near B_K the AMRO behavior is mixed. A similar diagram is observed for the M = Rb and Tl compounds .

FIG. 2. Temperature dependence of the resistance in α-$(ET)_2KHg(SCN)_4$ at zero magnetic field. Inside the normal metal state, $R(T) \propto T$. Inside DWI, $R(T) \propto \alpha T + \beta T^2$.

FIG. 3. (a) AMRO in α-$(ET)_2KHg(SCN)_4$ at 14 tesla and 2 K in DWI. (b) The temperature dependence for the field orientations marked by the arrows in (a). A metallic temperature dependence is observed when the field orientation corresponds to AMRO minima (curve D). On the other hand at AMRO maxima the behavior is nonmetallic (as seen in C, B, and A).

FIG. 4. Temperature dependence of the magnetoresistance in DWI at 14 tesla. At AMRO maxima the temperature dependence can be approximated to be proportional to τ. At AMRO minima the temperature dependence is approximated to be proportional to $1/\tau$ and T. R(T) at the AMRO minimum is fit to $A_1 + A_2T + A_3T^2$ and at AMRO maximum it is fit to $A_4/(A_5 + A_6T + A_7T^2)$, where A_1, A_2, A_3, A_4, A_5, A_6, and A_7 are constants.

FIG. 5. AMRO in α-$(ET)_2KHg(SCN)_4$ at 30 tesla and 0.5 K corresponding to the normal state and DWII (Left side). Temperature dependence of α-$(ET)_2KHg(SCN)_4$ magnetoresistance at various field positions as marked by arrows on the left side (Right side). A metallic temperature dependence is observed at AMRO minima (curve H) and a nonmetallic dependence at all other positions (curve G, F, and E). A reentrant metallic behavior is evident for positions corresponding to AMRO maxima below 3 K (inside DWII) (curve A).

FIG. 6. Temperature dependence of the magnetoresistance at 33 tesla. Anisotropic temperature dependence develops along with the AMRO. At AMRO maxima the temperature dependence is inversely proportional to T. The fit in the figure is $R(T)=A_1/\mathrm{T} + A_2$, where A_1 and A_2 are constants. At lowest temperatures the resistance starts to saturate and the fit fails. At AMRO minima the temperature dependence is proportional to T. The fit in the figure is $R(T)=A_3\mathrm{T} + A_4$, where A_3 and A_4 are constants.

FIG. 7. Temperature dependence of α-$(\mathrm{ET})_2\mathrm{TlHg(SCN)}_4$ in DWII near field orientations corresponding to AMRO maxima, reentrant metallic behavior is observed. Arrows mark the transition temperature T_M into this new metallic behavior. Both the slope of the temperature dependence and the value of T_M change with respect to field strength and orientation. a) 30 tesla data and b) 32.5 tesla data reveals the behavior clearly. The dashed lines are fits by assuming the conductivity is the sum of the $R(T,\theta)$ of the normal state plus a new angular independent metallic term (see text).

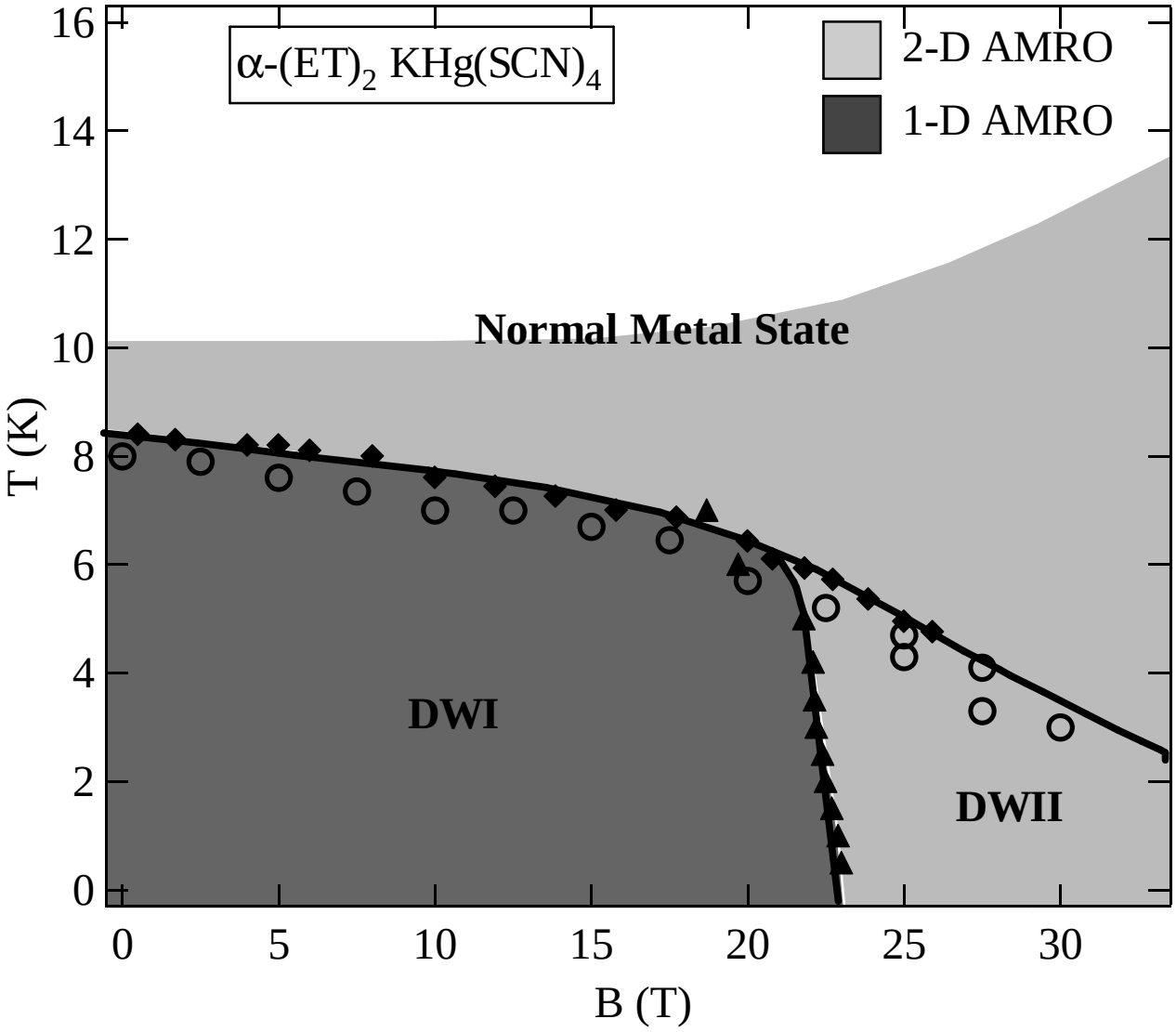
α-(ET)2 KHg(SCN)4
2-D AMRO
1-D AMRO
Normal Metal State
DWI
DWII
T (K)
B (T)
0
2
4
6
8
10
12
14
16
0
5
10
15
20
25
30

Fig. 1

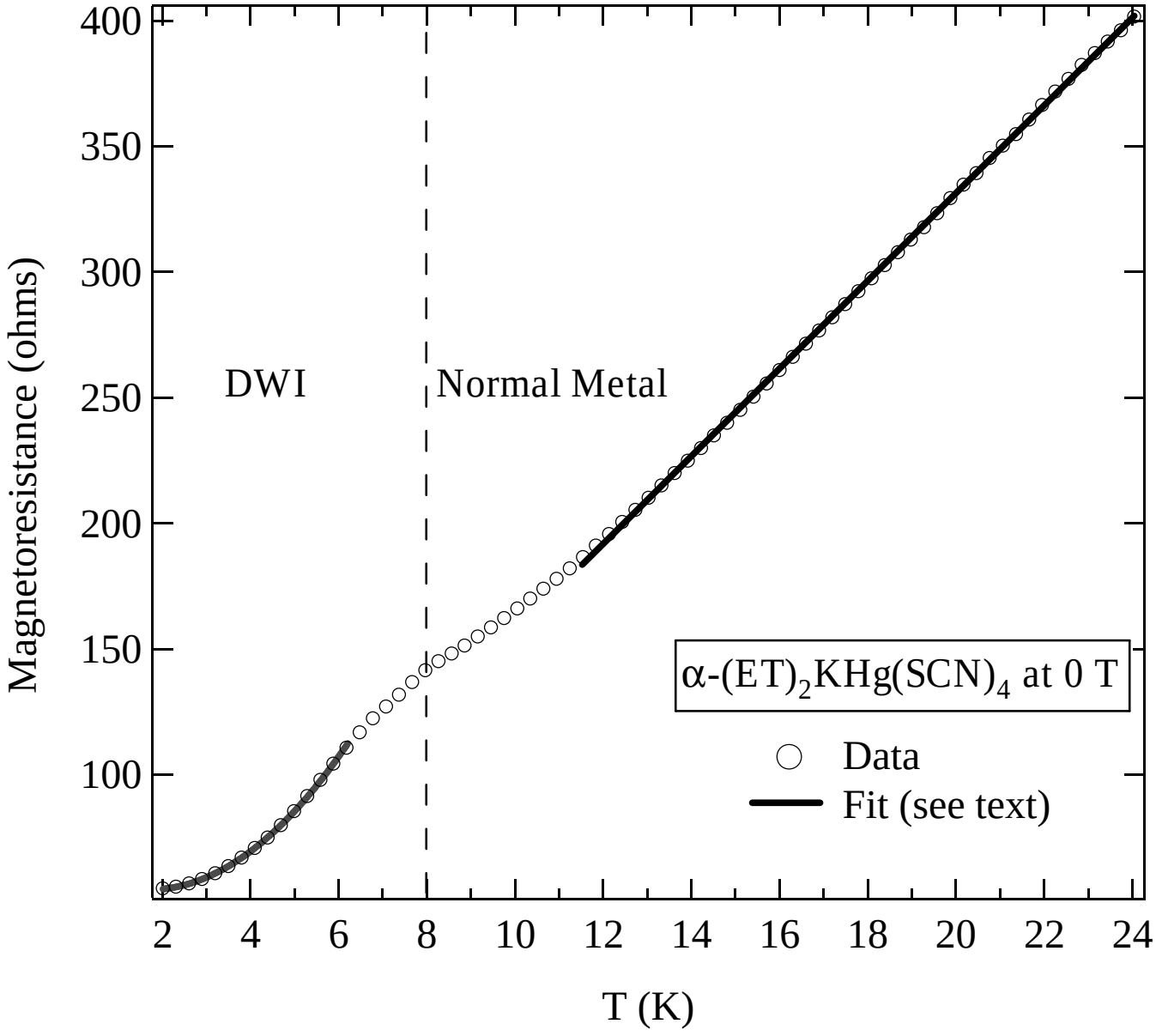
400
350
300
250
200
150
100
Magnetoresistance (ohms)
DWI
Normal Metal
α-(ET)2KHg(SCN)4 at 0 T
Data
Fit (see text)
2
4
6
8
10
12
14
16
18
20
22
24
T (K)

Fig. 2

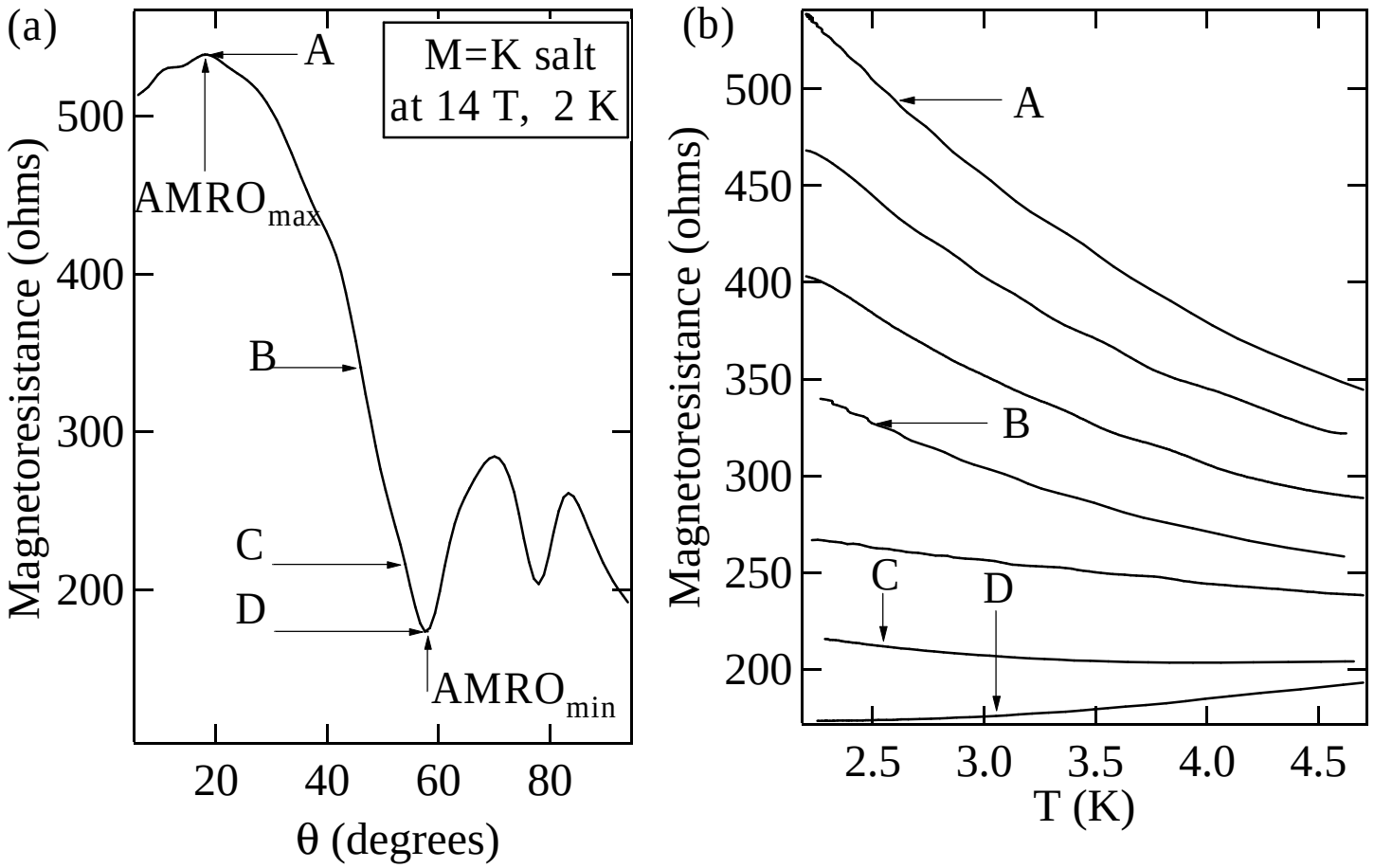
(a)
M=K salt
at 14 T, 2 K
A
B
C
D
AMRO$_{max}$
AMRO$_{min}$
Magnetoresistance (ohms)
500
400
300
200
20
40
60
80
θ (degrees)
(b)
A
B
C
D
Magnetoresistance (ohms)
500
450
400
350
300
250
200
2.5
3.0
3.5
4.0
4.5
T (K)

Fig. 3

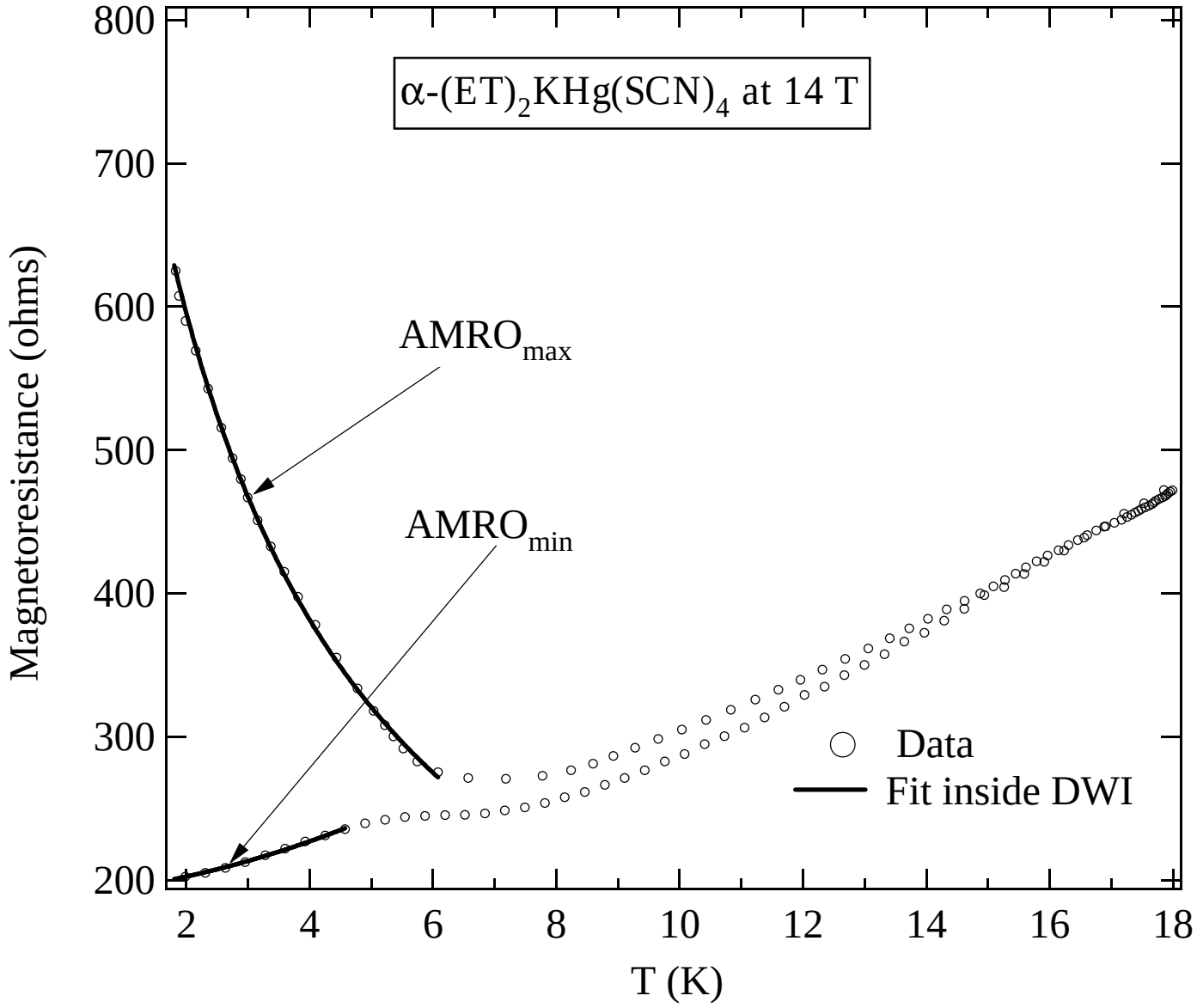
α-(ET)2KHg(SCN)4 at 14 T
AMROmax
AMROmin
Data
Fit inside DWI
Magnetoresistance (ohms)
T (K)
800
700
600
500
400
300
200
2
4
6
8
10
12
14
16
18

Fig. 4

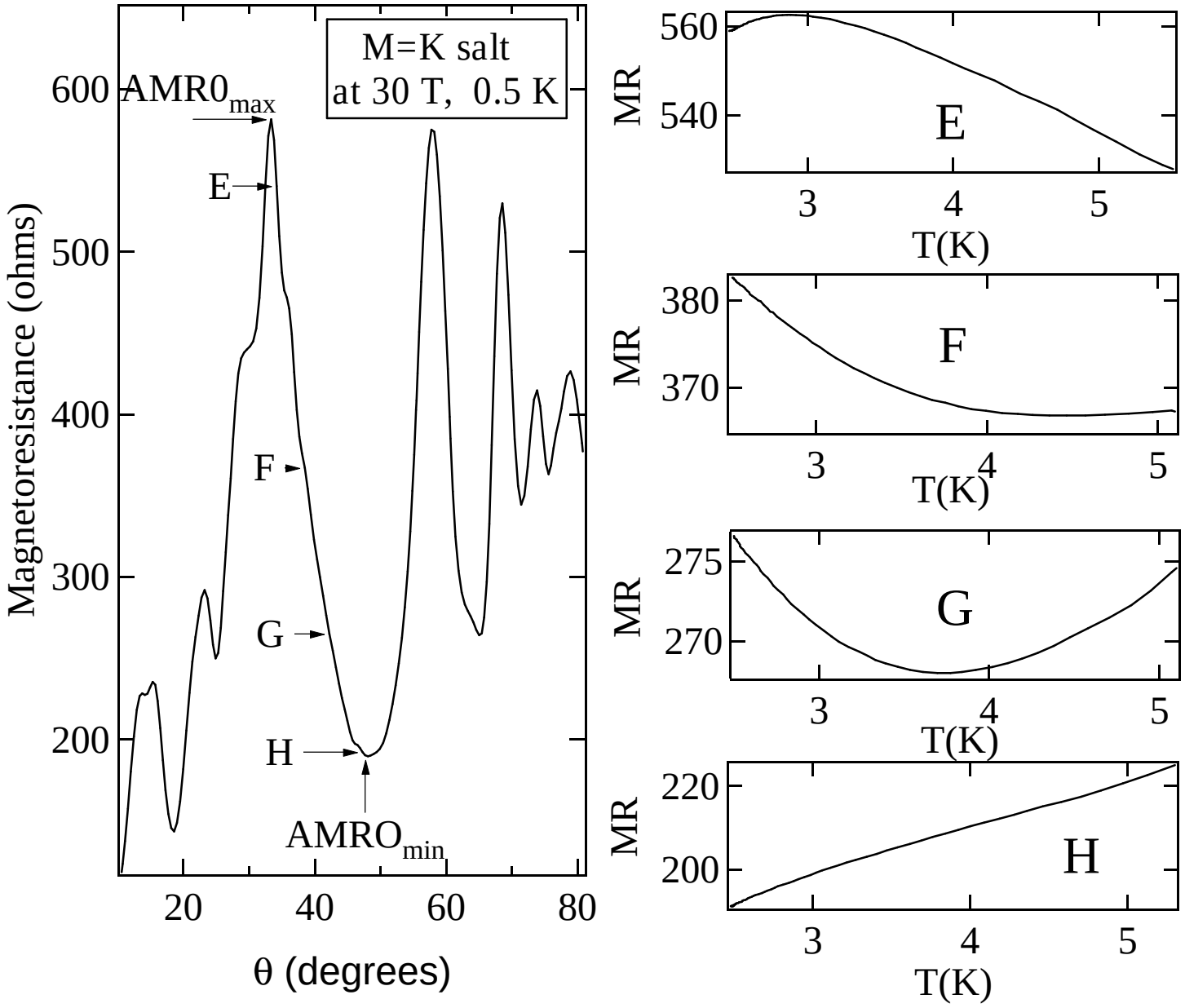
M=K salt
at 30 T, 0.5 K
AMR0max
E
F
G
H
AMRO min
Magnetoresistance (ohms)
θ (degrees)
MR
T(K)

Fig . 5

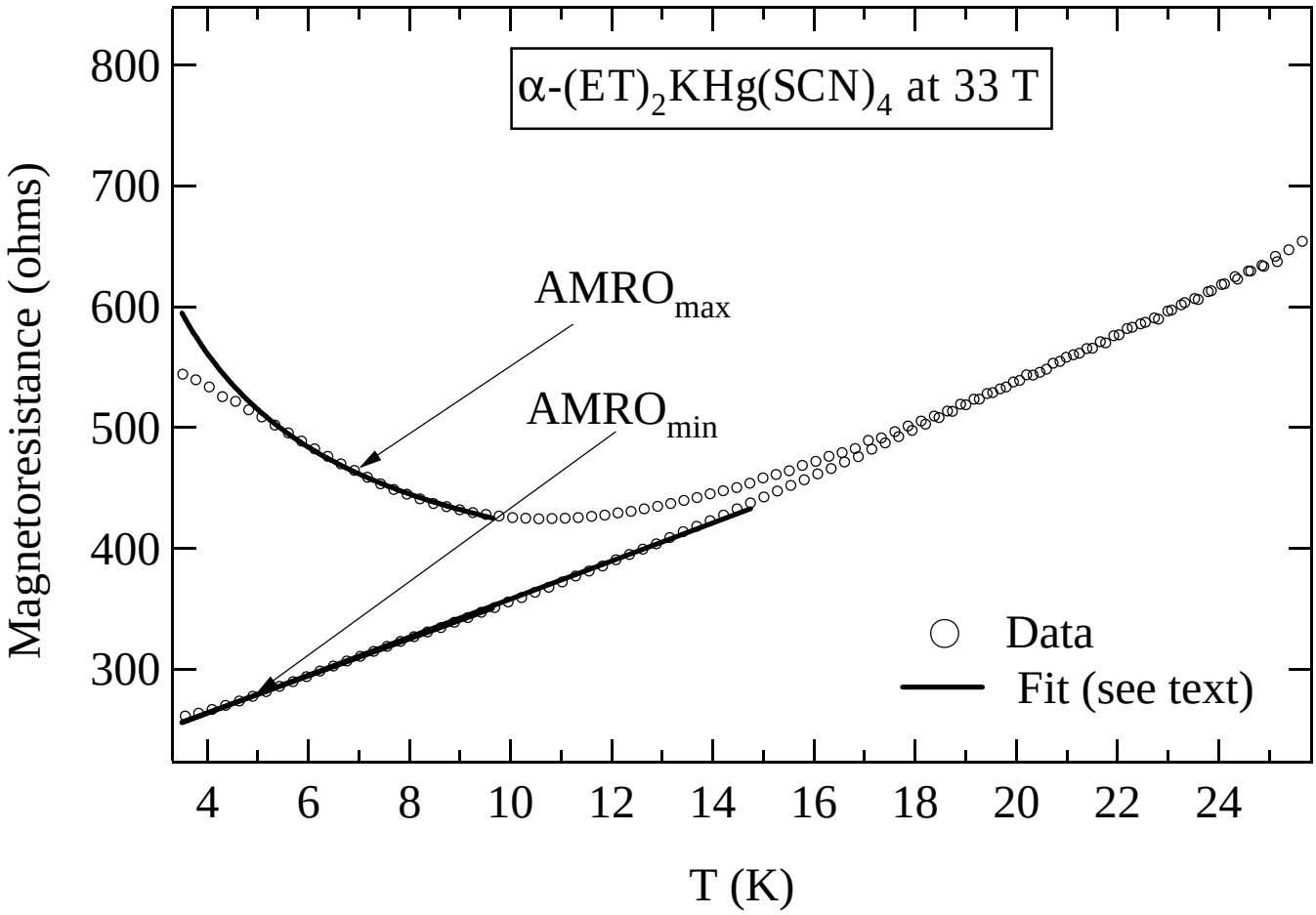
α-(ET)2KHg(SCN)4 at 33 T
AMROmax
AMROmin
Data
Fit (see text)
Magnetoresistance (ohms)
T (K)
800
700
600
500
400
300
4
6
8
10
12
14
16
18
20
22
24

Fig. 6

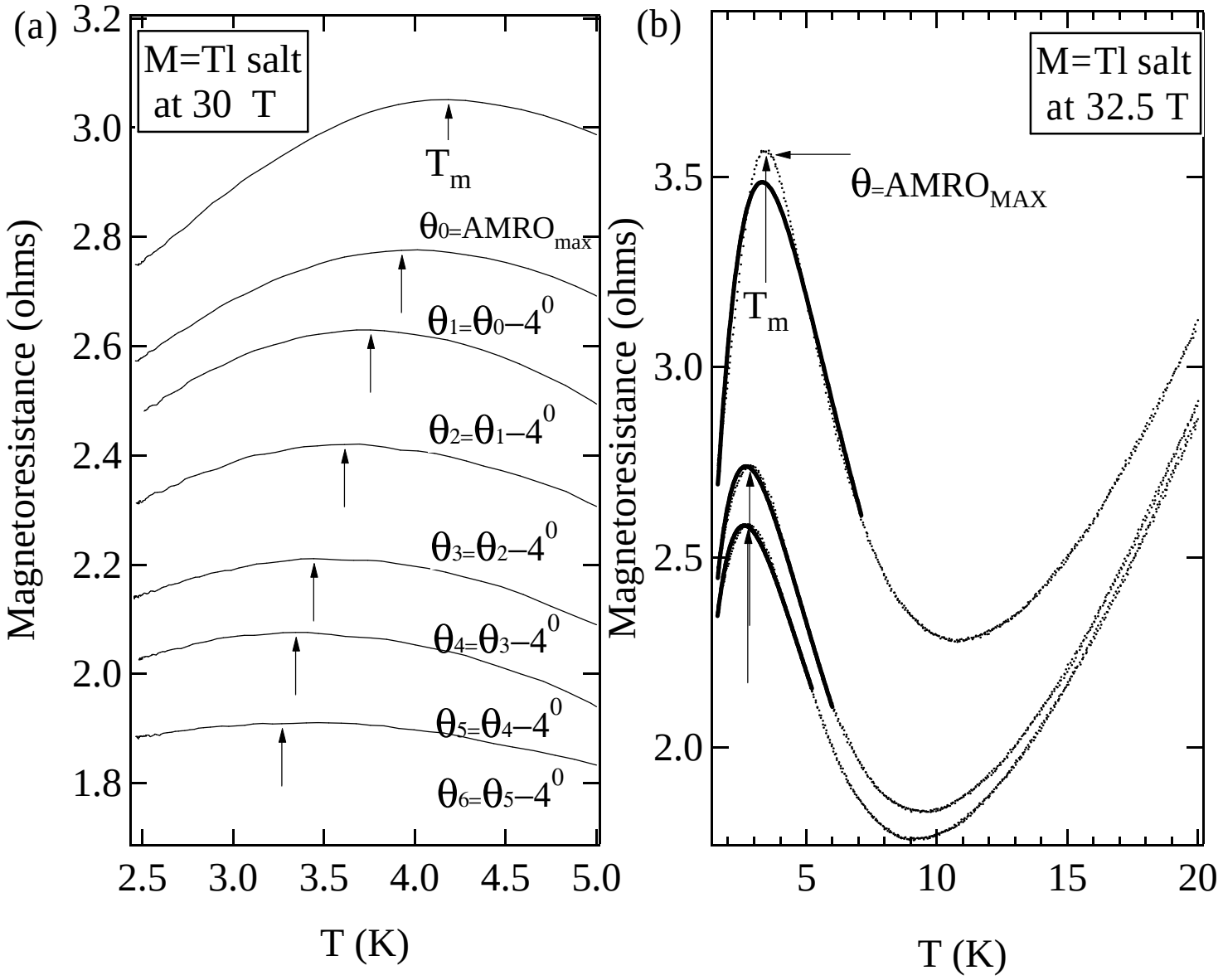
(a)
M=Tl salt
at 30 T
T_m
θ_0=AMRO$_{max}$
$\theta_1=\theta_0-4^0$
$\theta_2=\theta_1-4^0$
$\theta_3=\theta_2-4^0$
$\theta_4=\theta_3-4^0$
$\theta_5=\theta_4-4^0$
$\theta_6=\theta_5-4^0$
Magnetoresistance (ohms)
T (K)
(b)
M=Tl salt
at 32.5 T
θ=AMRO$_{MAX}$
T_m
Magnetoresistance (ohms)
T (K)

Fig. 7